Virus-SiO2 and Virus-SiO2-Au Hybrid Particles with Tunable Morphology

van Rijn, Patrick; van Bezouwen, Laura S.; Fischer, Rainer; Boekema, Egbert J.; Boeker, Alexander; Commandeur, Ulrich

Published in:
Particle & Particle Systems Characterization

DOI:
10.1002/ppsc.201400068

Publication date:
2015

Particle & Particle Systems Characterization
www.particle-journal.com

Virus-SiO_2 and Virus-SiO_2-Au Hybrid Particles with Tunable Morphology

Patrick van Rijn, Laura S. van Bezouwen, Rainer Fischer, Egbert J. Boekema, Alexander Böker, and Ulrich Commandeur**

Biohybrid materials combine different functional characteristics within a single and specific structural entity.[1–3] Plant viruses are particularly suitable for the development of such new materials.[4–7] They can be used as nanocontainers/reactors[8–12] or as templates for the placement of organic molecular components[13,14] and/or inorganic materials such as metals,[15–18] metal oxides,[19–21] and SiO_2, creating nano- and mesoscopic structures.[22–25] These functionalized virus particles can be used for drug delivery,[26,27] photonics,[28] sensing applications,[29] and as nanoelectronic devices.[30,31] Genetic engineering is a convenient way to add more functions to the virus structure in order to create hybrid materials,[32] for example, by adding peptide sequences that promote the formation of SiO_2 from organic–inorganic SiO_2 precursors as is seen in other biomineralization systems.[33–35] This approach has been used to coat the rigid rod-shaped structure of *Tobacco mosaic virus* (TMV), as well as small spherical *Cowpea mosaic virus* (CPMV) particles, with a homogeneous dense layer of SiO_2.[22–25]

Rod-shaped particles can have a larger surface area than globular particles without losing one of the dimensions in the lower nanometer range because of the one dimensional increase in size making the rigid rods such as TMV more attractive than the globular particles such as CPMV. Additionally, both are stable under extreme pH, temperature or co-solvent conditions, but the particles with greater flexibility such as *Potato Virus X* (PVX) makes them interesting as potential biomarkers[36–38] or scaffolds for biocatalysts,[39] albeit at the expense of stability as determined by comparative differential scanning calorimetry (DSC) studies.[40] It is important to extrapolate procedures towards different types of viral structures due to the difference in size, mechanical properties, and chemical addressability. The different sizes and shapes bring forth new structures as was shown using the extremely long and flexible *M13 fd phage* (880 nm long, 7 nm wide) in comparison with TMV, which is much shorter (300 nm) and wider (18 nm) hence more rigid. With similar silicification approaches, these gave completely different architectures, namely bundled fibers and small star-shaped nanoparticles, respectively, of which the latter only displayed these structure with the smaller broken TMV fragments.[22] The dimension of PVX is in between the two frequently used M13 and TMV structures and displays intermediate length (515 nm) as well as width (13 nm) with still a high degree of flexibility. By using such an intermediate structure, new structures and morphologies are expected, broadening the scope and applicability of engineered viruses in material science in combination with processes such as biomineralization.[24,41,42]

We introduced the peptide sequence YSDQPTQSSQRP, known to induce SiO_2-formation,[24] onto the surface of PVX particles via genetic modification allowing them to be coated with inorganic material. PVX is the type member of the Potexvirus group. The particles are flexible rods 515 nm long and 13 nm wide, consisting of 1270 identical 25-kDa coat protein (CP) subunits. We coated the virus particles under mild conditions (pH-neutral aqueous solution at room temperature), which led to the formation of diverse hybrid and even triple-hybrid structures. While conventionally, the virus particles are homogeneously coated, we found that under the synthetic conditions as we present in this work, isolated SiO_2-nanoparticles were formed on the surface of the PVX, which allows the surface to be addressed even further via immunolabeling procedures. The antibody labeling approach is not possible in homogeneously coated virus particle systems and offers an additional modification tool in combination with the mineralization process. Using mixtures of different organo-silane precursors, the interactions with peptide-based structures can be influenced as was previously shown via incorporation of enzymes in porous silicon dioxide structures.[43] Mixing (3-aminopropyl)triethoxysilane (APTES) with tetraethylorthosilane (TEOS) provides mesoporous silicon dioxide structures.[44] Using the genetically modified PVX particles to induce the mineralization process, a complex 3-D super-structure of 1–2 μm in diameter was

Dr. P. van Rijn, Prof. A. Böker
Leibniz-Institut für Interaktive Materialien
Lehrstuhl für Makromolekulare
Materialien und Oberflächen
RWTH Aachen University
Germany Forckenbeckstrasse 50
52056 Aachen, Germany
E-mail: p.van.rijn@umcg.nl
Dr. P. van Rijn
University of Groningen
University Medical Center Groningen
BioMedical Engineering FB40
W. J. Kolff Institute for Biomedical Engineering and Materials Science
A. Deusinglaan 1, 9713 AV Groningen
The Netherlands
L. S. van Bezouwen, Prof. E. J. Boekema
Groningen Biomolecular Sciences and Biotechnology Institute
University of Groningen
Nijenborgh 7, 9747 AG Groningen
The Netherlands
Prof. R. Fischer, Dr. U. Commandeur
Institute of Biology VII, Molecular Biotechnology
RWTH Aachen University
Worringerweg 1, 52074 Aachen, Germany
Fax: (+)49-241-871062
E-mail: commandeur@molbiotech.rwth-aachen.de

DOI: 10.1002/ppsc.201400068

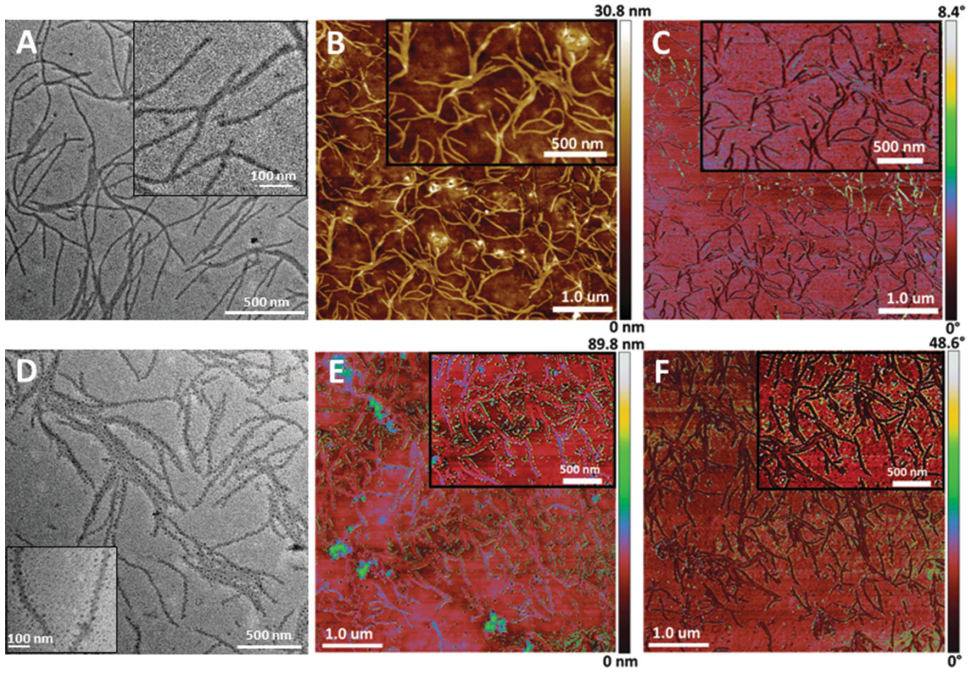

Figure 1. Structural determination following the silicification of wild-type PVX and engineered PVX-SIL particles. Wild-type PVX and PVX-SIL (1 mg mL^{-1} in MilliQ-water) was mixed with 2 µL mL^{-1} TEOS, sonicated briefly three times and left for 3 d. A/D) TEM and B/E) SFM (height), C/F) (phase)) analysis showed no structural changes to the wild-type particles and no SiO_2 deposits A–C) but the presence of SiO_2 particles (≈10 nm) distributed along the surface of the PVX-SIL particles, although not in a dense layer D–F). Color coding of SFM images was chosen to maximize difference in contrast.

formed, comprising of several PVX rods radiating from a central mesoporous silicon dioxide core.

Most procedures for coating viruses with inorganic materials require additional reducing agents, reactants, or co-solvents. A simple approach has previously been used to coat CPMV particles homogeneously, although the reaction was carried out at 45 °C, which is unsuitable for PVX particles due to their lower stability.[22–25] Therefore we mixed 1 mg mL^{-1} of genetically engineered "PVX for silicification" (PVX-SIL) in Millipore water with 2 µL mL^{-1} TEOS followed by three 10-seconds bursts of sonication interspersed with vigorous shaking (vortex, 1500 rpm). The reaction mixture was then left undisturbed for 3 d at room temperature. Wild-type PVX particles were used as a control. The reaction mixture with wild-type PVX and TEOS produced uncoated wild-type PVX particles (**Figure 1**A–C), but the PVX-SIL particles were covered with small SiO_2 nanoparticles along their length as revealed by transmission electron microscopy (TEM) and the phase image obtained by scanning force microscopy (SFM) (Figure 1D–F).

The PVX-SIL template is not uniformly coated with SiO_2 but instead isolated SiO_2 nanoparticles are formed, which leaves parts of the surface of the virus particle still accessible. This allowed other targeting methods to be applied, such as immunolabeling with monoclonal gold-conjugated antibodies to target the PVX surface and create a triple-hybrid system composed of a self-assembled PVX core coated with semiconducting SiO_2 nanoparticles and conductive gold nanoparticles. On-grid labeling experiments with antibody-conjugated gold nanoparticles confirmed that the SiO_2-coated PVX-SIL surface was still accessible for additional labeling (**Figure 2**). The gold nanoparticles attached over the entire length of the PVX particle, confirming that the original SiO_2 nanoparticles did not form a uniform dense layer. The SiO_2 particles were more difficult to see in the triple-hybrid structure because the gold particles have a much higher contrast. In principle, any type of particle can be added during the second labeling step, for example, silver, platinum or quantum dots, as long as they are conjugated to an appropriate antibody. The additional gold nanoparticles seen in between the PVX particles are due to the procedure of on-grid labeling.

We anticipated that changing the silicon dioxide precursor would affect the mineralization process as was also observed previously[45] and provide additional tools for further modification of both the overall structure and the silicon dioxide

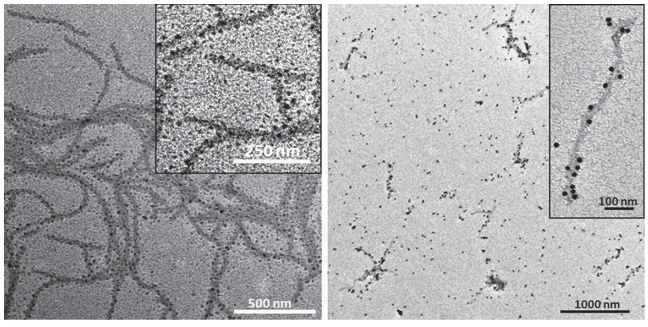

Figure 2. Double labeling of PVX-SIL virus particles. PVX-SIL (1 mg mL^{-1} in MilliQ-water) was mixed with 2 µL mL^{-1} TEOS, sonicated briefly and left for 3 d (left panel). The coated particles were then immunolabeled with gold nanoparticles to generate a triple-hybrid virus-silica-gold structure (right panel).The defined SiO_2 particles cannot be distinguished separately due to the high contrast of the gold nanoparticles.

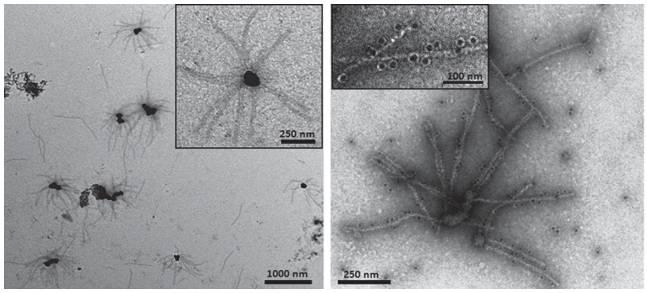

Figure 3. PVX-SiO_2 superstructures. PVX-SIL particles (1 mg mL^{-1} in MilliQ-water) were mixed with 2 µL mL^{-1} of a 1:1 mixture of TEOS and APTES, sonicated briefly three times and left for 3 d at room temperature. TEM analysis revealed large structures with a dense core radiating PVX-SIL filaments (left panel) that were still accessible for immunogold labeling (right panel).

morphology itself. We therefore mixed TEOS with an equal volume of APTES and repeated the earlier labeling experiments using 2 µL mL^{-1} of the silicification mixture. The TEOS/APTES mixture gave rise to viral-silicon dioxide superstructures. The mineralization process was not confined to the surface of the virus particles. Instead, independent nucleation sites arose spontaneously, to which the ends of the PVX-SIL particles became attached to generate a mesoporous silicon dioxide core with radiating PVX tentacles (**Figure 3**).

Most likely, as in other investigations with enzymes where the addition of the amine-functionality to the system via co-condensation along with TEOS facilitates coordination of the protein structures via electrostatic interactions also applies for the PVX particle.[43] It is envisioned that due to the mesoporous nature of the large silicon dioxide core, the elongated structure of the PVX particles fits into it and hence becomes confined. The mesoporous nature of the core as well as the fact that indeed the structure is 3D, was indicated by cryo-TEM (**Figure 4**). The enhanced contrast obtained from cryo-TEM shows that the core is of nonhomogenous density, providing a qualitative indication of the mesoporosity and is in accordance with other systems as mentioned before. Although, the combinations with APTES are known to provide mesoporous particles, it was not determined to what extend the entrapped virus particles add to the porosity or whether the porosity was solely due to the presence of the virus-ends inside the core. The 3D nature of the structure is shown by tilting the sample by 45° in opposite directions (Figure 4C–E). It is seen that the PVX particles, which are protruding from the core move away from under the core structure, strongly indicating that the overall particle is 3D (indicated by the arrows in Figure 4C–E). Again, the wild-type PVX did not undergo any form of mineralization and the superstructures did not form with TEOS alone. In previous studies, such superstructures of these dimensions required a combination of techniques to increase the affinity of the filament ends for the silica matrix, for example, through biotin–streptavidin affinity binding.[46] In order to investigate whether the entrapment of the PVX is via incorporation into the mesoporous core structure or that there is a specific affinity for the ends of the PVX structures towards the silicon dioxide core, end-labeling experiments have been performed. End-labeling experiments via immunogold labeling did not distinguish any difference between the proximal and distal ends of the PVX-SIL particle and therefore support the inclusion of the PVX into the mesoporous network although it has to be noted that these findings are not conclusive (S2, Supporting Information). The PVX-SiO_2 superstructures were purified via repeated mild centrifugation, washing, and redispersion.

Although the PVX-SiO_2 superstructure has a complex morphology and chemical composition, we also considered additional labeling as discussed above for the individual SiO_2-particle-coated PVX-SIL virus particle. Similarly, we found that the surface of the PVX-SIL particles radiating from the core remained accessible to immunogold labeling, resulting in the creation of triple-hybrid superstructures containing both SiO_2 and gold (Figure 3).

The composition of the silicon oxide precursors dictates the morphology of the hybrid structures, which was also shown when instead of APTES, iodopropyltriethoxysilane (IPTOS) was added to induce hydrophobicity on the silicon oxide structures formed in combination with the PVX-SIL virus particles. The importance of the appropriate composition is reflected by the complete lack of structure and very unspecific silicification when a combination of TEOS/IPTOS (1:1) was used (S3, Supporting Information).

We have shown that filamentous, anisotropic, flexible plant viruses offer a versatile platform for the formation of complex

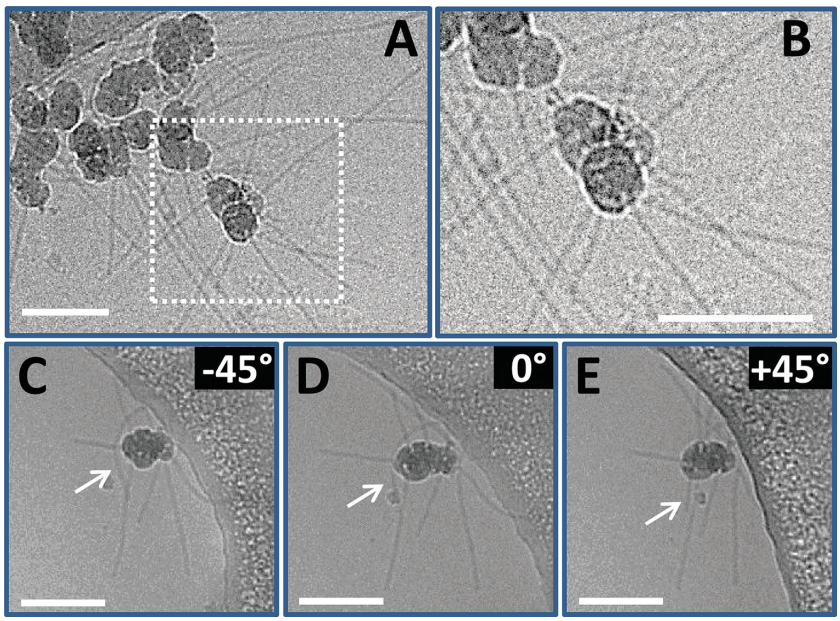

Figure 4. A–E) Cryo-TEM images of PVX-SiO_2 superstructures. The core that holds the PVX structures displays an inhomogeneous structuring indicating the mesoporous morphology (A/B). C–E) By tilting the image, the 3D nature of the particle is displayed. The presence of SiO_2 was shown by EDX analysis done with regular TEM (S1, SupportingInfo rmation).

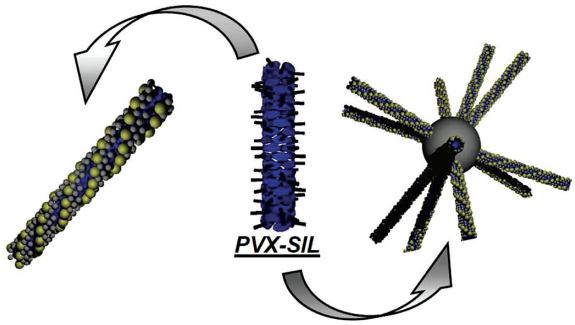

Scheme 1. Engineered PVX particles with flexible filaments provides a platform for the development of hybrid and triple hybrid materials. Here, a combination of SiO_2-based precursors and immunogold labeling was used but different engineered peptides can in principle be used to achieve coating with other semiconductors and metals as well as changing the monoclonal gold-conjugated antibodies could be replaced with any other type of labeled monoclonal antibody to increase the versatility of the hybrid structures.

hybrid materials including isolated coated virus particles and complex microstructures. These structures formed under mild conditions making them suitable for more delicate viral particles. Similar processes have been explored using globular viruses and stable rigid rods, predominantly yielding isolated fully-covered virus particles. By changing the engineered peptide, it should be possible to achieve the condensation of other semiconductor materials or metals, thus expanding the properties and versatility of the hybrid materials (**Scheme 1**). Furthermore, the ability to combine silicification with immunolabeling (also under mild conditions) provides a straightforward method to develop triple-hybrid complex structures, whose material composition and functional properties are controllable.

Experimental Section

Materials: Unless otherwise stated, all chemicals were purchased from Sigma–Aldrich and were used without further purification. PVX particles were end-labeled with a murine monoclonal anti-PVX antibody combined with a goat anti-mouse IgG labeled with 15-nm gold particles (BB International).[47] Chemicals were mixed using a Bandelin Sonorex operating at 35 kHz and an IKA Vortex Genius 3 operating at 2500 rpm. For TEM imaging, a drop of solution was placed on a carbon-coated copper grid and excess liquid was removed after 2 min. Immunogold labeling was carried out with a polyclonal anti-PVX antibody (DSMZ, Germany) combined with a goat anti-rabbit IgG labeled with 15-nm gold particles (BB International). TEM images were captured on a ZEISS LIBRA120 PLUS electron microscope, operating at 80 kV. Cryo-SEM samples were placed on carbon-coated grids and plunged in liquid nitrogen. The images were captured after partial surface sublimation using a Hitachi S-4800 field-emission scanning electron microscope (FESEM) operating at 1–2 kV and 10 μA. Scanning force microscopy images were captured in tapping mode on a Veeco Instruments Scanning Force Microscope operating on Nanoscope software.

Samples for cryo-TEM were prepared by deposition of a few microliters of the virus and silica solution on the holey carbon-coated grids (Quantifoil 3.5/1, Quantifoil Micro Tools). After blotting of the excess liquid, the grids were vitrified in liquid ethane in a Vitrobot (FEI) and transferred to a Philips Technai 20 cryo-electron microscope equipped with a Gatan model 626 cyro-stage, operating at 200 kV. Images were recorded under low-dose conditions with a slow-scan CCD camera. Detection of elements by EDX has been done with an Oxford X-Max 80 Silicon drift EDX detector with regular TEM. INCA software was used for analysing the data.

Expression Vector Construction and Plant Infection: The PVX-derived plant expression vector was modified with the silicification peptide coding sequence as a 5′-end translational fusion with the CP gene resulting in a direct N-terminal CP fusion. The silicification peptide coding sequence was included into primer sequences that also incorporated restriction sites suitable for cloning into the expression vector. Following amplification, the PCR product was digested using specific restriction enzymes and cloned into the expression vector, which had been prepared using the same enzyme set. Plasmid DNA used for plant infection was amplified in *Escherichia coli* strain DH5α.

The recombinant PVX vector was used for DNA inoculation of individual *N. benthamiana* plants. Plants were inoculated by gentle abrading the surfaces of three leaves per plant with carborundum and 5 μg of plasmid DNA as described elsewhere.[41] Plants were grown with 16 h light (25.-30.000 lux) at 25 °C, 8 h dark at 20 °C and 60% humidity.

Preparation of PVX-SIL Mutant Particles: PVX-SIL particles bearing the silicification peptide YSDQPTQSSQRP were purified using a modified CIP protocol (International Potato Center, Lima, Peru) based on PEG precipitation followed by sucrose gradient centrifugation (http://www.cipotato.org/training/Materials/PVTechs/Fasc5.2(99).pdf). Briefly, 100 g of systemically infected leaf material stored at −80 °C was homogenized in 2 volumes of ice-cold 0.1 M phosphate buffer (pH 8.0) containing 10% ethanol and the mixture was supplemented with 0.2% 2-mercaptoethanol prior to filtration through three layers of gauze. Cellular debris was removed by centrifugation (30 min, 7800 × g, 4 °C) and the supernatant was supplemented with 1% Triton X-100. The solution was stirred for 1 h at 4 °C and clarified by centrifugation (20 min, 5500 × g, 4 °C). The supernatant was supplemented with 0.2 M NaCl and 4% PEG (MW 6000–8000). The mixture was stirred for 1 h at 4 °C and incubated for 1 h at room temperature. After clarification by centrifugation (30 min, 7800 × g), the pellet was resuspended in 6 mL 0.05 M phosphate buffer (pH 8.0) with 1% Triton X-100 overnight at 4 °C, and clarified again by centrifugation (10 min, 7800 × g). The cleared solution was loaded onto a 10%–45% sucrose gradient in 0.01 M phosphate buffer (pH 7.2) containing 0.01 M EDTA. After further centrifugation (75 min, 96,500 × g, 4 °C), the virus band was removed with a syringe along with adjacent 1.5 mL fractions. Sucrose gradient fractions containing PVX-SIL particles, as verified by sodium dodecylsulfate polyacrylamide gel electrophoresis (SDS-PAGE), were combined, diluted with the same volume of 0.01 M phosphate buffer (pH 7.2) and centrifuged at least for 3 h at 102,600 × g, at 4°C. The pellets were dissolved by continuous stirring in 0.2 mL 0.01 M phosphate buffer (pH 7.2) overnight, and after clarification by centrifugation (6 min, 5000 × g, 4 °C), the concentration of purified virus particles was calculated using the PVX extinction coefficient (2.97) for the extinction values at 260 nm. Peptide insertion was confirmed by SDS-PAGE and the particles were characterized by TEM (as described in S4, Supporting Information).

Immunogold Labeling: PVX particles were labeled directly on the carbon-coated copper grid using 1 μL of the reaction solution diluted in 9 μL of MilliQ water.[48] After 2 min, the excess solution was removed and the grid was incubated for 2 h with the primary antibody (see materials) diluted to 20 ng μL^{-1} in phosphate-buffered saline (pH 7.0). The grid was then washed with 20 drops of PBST buffer, the excess solution was removed, and the grid was then incubated for 2 h with the secondary antibody (see materials) diluted to ≈0.25 ng μL^{-1} in PBS (pH 7.0). The grid was then washed twice with 20 drops of phosphate-buffered saline (pH 7.0) containing 0.05 wt% Tween-20, and then twice with 20 drops of distilled water. The excess solution was removed prior to imaging.

Supporting Information

Supporting Information is available from the Wiley Online Library or from the author.

Acknowledgements

The authors thank Karolin Richter for excellent technical assistance.

Received: April 3, 2014
Revised: June 30, 2014
Published online: August 5, 2014

[1] P. van Rijn, A. Böker, *J. Mater. Chem.* **2011**, *21*, 16735.
[2] G. Jutz, A. Böker, *Polymer.* **2011**, *52*, 211.
[3] L. A. Lee, H. G. Nguyen, Q. Wang, *Org. Biomol. Chem.* **2011**, *9*, 6189.
[4] S.-Y. Lee, J.-S. Lim, M. T. Harris, *Biotechnol. Bioeng.* **2012**, *109*, 16.
[5] M. Young, D. Willits, M. Uchida, T. Douglas, *Annu. Rev. Phytopathol.* **2008**, *46*, 361.
[6] T. Douglas, M. Young, *Science.* **2006**, *312*, 873.
[7] D. J. Evans, *J. Mater. Chem.* **2008**, *18*, 3746.
[8] A. de la Escosura, R. J. M. Nolte, J. J. L. M. Cornelissen, *J. Mater. Chem.* **2009**, *19*, 2274.
[9] T. Douglas, M. Young, *Nature* **1998**, *393*, 152.
[10] A. de la Escosura, P. G. A. Janssen, A. P. H. J. Schenning, R. J. M. Nolte, J. J. L. M. Cornelissen, *Angew. Chem. Int. Ed.* **2010**, *49*, 5335.
[11] M. A. Kostiainen, O. Kasyutich, J. J. L. M. Cornelissen, R. J. M. Nolte, *Nat. Chem.* **2010**, *2*, 394.
[12] M. Comellas-Aragonès, H. Engelkamp, V. I. Claessen, N. A. J. M. Sommerdijk, A. E. Rowan, P. C. M. Christianen, J. C. Maan, B. J. M. Verduin, J. J. L. M. Cornelissen, R. J. M. Nolte, *Nat. Nanotechnol.* **2007**, *2*, 635.
[13] R. A. Miller, A. D. Presley, M. B. Francis, *J. Am. Chem. Soc.* **2007**, *129*, 3104.
[14] M. A. Bruckman, G. Kaur, L. A. Lee, F. Xie, J. Sepulveda, R. Breitenkamp, X. Zhang, M. Joralemon, T. P. Russell, T. Emrick, Q. Wang, *ChemBioChem* **2008**, *9*, 519.
[15] A. Aljabali, F. Sainsbury, G. P. Lomonossoff, D. J. Evans, *Small* **2010**, *6*, 818.
[16] K. M. Bromley, A. J. Patil, A. W. Perriman, G. Stubbs, S. Mann, *J. Mater. Chem.* **2008**, *18*, 4796.
[17] M. T. Lee, S.-Y. Choi, J. Royston, E. Janes, D. B. Culver, J. N. Harris, *J. Nanosci. Nanotechnol.* **2006**, *6*, 974.
[18] C. Mao, D. J. Solis, B. D. Reiss, S. T. Kottmann, R. Y. Sweeney, A. Hayhurst, G. Georgiou, B. Iverson, A. M. Belcher, *Science.* **2004**, *303*, 213.
[19] C. Jolley, M. Klem, R. Harrington, J. Parise, T. Douglas, *Nanoscale* **2011**, *3*, 1004.
[20] T. Douglas, M. Young, *Adv. Mater.* **1999**, *11*, 679.
[21] P. Atanasova, D. Rothenstein, J. J. Schneider, R. C. Hoffmann, S. Dilfer, S. Eiben, C. Wege, H. Jeske, J. Bill, *Adv. Mater.* **2011**, *23*, 4918.
[22] E. Royston, S.-Y. Lee, J. N. Culver, M. T. Harris, *J. Colloid. Interface Sci.* **2006**, *298*, 706.
[23] E. S. Royston, A. D. Brown, M. T. Harris, J. N. Culver, *J. Colloid. Interface Sci.* **2009**, *332*, 402.
[24] N. F. Steinmetz, S. N. Shah, J. E. Barclay, G. Rallapalli, G. P. Lomonossoff, D. J. Evans, *Small* **2009**, *5*, 813.
[25] Z. Zhang, J. Buitenhuis, *Small* **2007**, *3*, 424.
[26] Z. Wu, K. Chen, I. Yildiz, A. Dirksen, R. Fischer, P. E. Dawson, N. F. Steinmetz, *Nanoscale* **2012**, *4*, 3567.
[27] J. D. Lewis, G. Destito, A. Zijlstra, M. J. Gonzalez, J. P. Quigley, M. Manchester, H. Stuhlmann, *Nat. Med.* **2006**, *12*, 354.
[28] S. K. Dixit, N. L. Goicochea, M.-C. Daniel, A. Murali, L. Bronstein, M. De, B. Stein, V. M. Rotello, C. C. Kao, B. Dragnea, *Nano Lett.* **2006**, *6*, 1993.
[29] C. Mao, A. Liu, B. Cao, *Angew. Chem. Int. Ed.* **2009**, *48*, 6790.
[30] R. J. Tseng, C. Tsai, L. Ma, J. Ouyang, C. S. Ozkan, Y. Yang, *Nat. Nanotechnol.* **2006**, *1*, 72.
[31] B. Y. Lee, J. Zhang, C. Zueger, W.-J. Chung, S. Y. Yoo, E. Wang, J. Meyer, R. Ramesh, S.-W. Lee, *Nat. Nanotechnol.* **2012**, *7*, 351.
[32] L. Shen, N. Bao, Z. Zhou, P. E. Prevelige, A. Gupta, *J. Mater. Chem.* **2011**, *21*, 18868.
[33] J. K. Pokorski, N. F. Steinmetz, *Mol. Pharm.* **2011**, *8*, 29.
[34] T. M. Garakani, H. Wang, T. Krappitz, B. M. Liebeck, P. van Rijn, A. Böker, *Chem. Commun.* **2012**, *48*, 10210.
[35] A. Schulz, H. Wang, P. van Rijn, A. Böker, *J. Mater. Chem.* **2011**, *21*, 18903.
[36] N. F. Steinmetz, M. E. Mertens, R. E. Taurog, J. E. Johnson, U. Commandeur, R. Fischer, M. Manchester, *Nano Lett.* **2010**, *10*, 305.
[37] S. Shukla, A. M. Wen, N. R. Ayat, U. Commandeur, R. Gopalkrishnan, A.-M. Broome, K. W. Lozada, R. A. Keri, N. F. Steinmetz, *Nanomedicine* **2013**, *9*, 221.
[38] K. L. Lee, K. Uhde-holzem, R. Fischer, U. Commandeur, N. F. Steinmetz, in *Virus Hybrids as Nanomaterials—Methods and Protocols* (Eds: B. Lin, B. Ratna), Humana Press, Totowa, NJ **2014**, pp. 3.
[39] N. Carette, H. Engelkamp, E. Akpa, S. J. Pierre, N. R. Cameron, P. C. M. Christianen, J. C. Maan, J. C. Thies, R. Weberskirch, A. E. Rowan, R. J. M. Nolte, T. Michon, J. C. M. Van Hest, *Nat. Nanotechnol.* **2007**, *2*, 226.
[40] V. N. Orlov, S. V Kust, P. V Kalmykov, V. P. Krivosheev, E. N. Dobrov, V. A. Drachev, *FEBS Lett.* **1998**, *433*, 307.
[41] C. M. Soto, B. R. Ratna, *Curr. Opin. Biotechnol.* **2010**, *21*, 426.
[42] B. C. E. Fowler, W. Shenton, G. Stubbs, S. Mann, *Adv. Mater.* **2001**, *13*, 1266.
[43] C. Lei, Y. Shin, J. Liu, E. J. Ackerman, *J. Am. Chem. Soc.* **2002**, *124*, 11242.
[44] T. M. Suzuki, T. Nakamura, K. Fukumoto, M. Yamamoto, Y. Akimoto, K. Yano, *J. Mol. Catal. A Chem.* **2008**, *280*, 224.
[45] E. Royston, S.-Y. Lee, J. N. Culver, M. T. Harris, *J. Colloid Interface Sci.* **2006**, *298*, 706.
[46] A. Mueller, F. J. Eber, C. Azucena, A. Petershans, A. M. Bittner, H. Gliemann, H. Jeske, C. Wege, *ACS Nano* **2011**, *5*, 4512.
[47] J. C. Farm, S. S. R. Estonian, *J. Gen. Virol.* **1988**, *69*, 1799.
[48] K. Uhde, R. Fischer, U. Commandeur, *Arch. Virol.* **2005**, *150*, 327.